Formation of homo- and heteronuclear complexes of 1-hydroxyethylidene-1,1-diphosphonic acid with Mn^{II} and Fe^{III} in aqueous solutions

F. V. Devyatov, O. V. Bogatyrev, and K. A. Ignat´eva*

Kazan (Volga region) Federal University,
18 ul. Kremlevskaya, 420008 Kazan, Russian Federation.
Fax: +7 (843) 233 7796. E-mail: olbogatyrev@gmail.com

Systems based on 1-hydroxyethylidene-1,1-diphosphonic acid (HEDP), iron(III)—HEDP and manganese(II)—iron(III)—HEDP, were studied by pH-potentiometry combined with mathematical modeling and NMR. Diverse and highly stable heteronuclear iron manganese complexes were found to exist in the heteronuclear system. The formation of the $MnH_3L_2^{3-}$, $FeMnH_3L_2^0$, $Fe_2MnHL_3^{3-}$, and MnL^{2-} complexes was established. The relaxation efficiency coefficient REC_2 (relaxivity) of these complexes was evaluated at ~2000 mol^{-1} s^{-1} L. Therefore, these systems hold promise as MRI contrast agents.

Key words: bisphosphonates, 1-hydroxyethylidene-1,1-diphosphonic acid, complexation, contrast agents, manganese(II), iron(III), MRI, NMR.

Stable paramagnetic complexes have attracted interest due their possible applications as magnetic resonance imaging (MRI) contrast agents.[1] Magnetic resonance imaging relies on the ability of some agents containing paramagnetic ions (Mn^{II} and Fe^{III}) to dramatically decrease water proton NMR relaxation times (T_1 and T_2). A decrease in these values leads to an increase in the information content of MRI studies.

The tumor uptake of a contrast agent can lead to either an increase or decrease in the proton signal intensity compared to the intensity outside the tumor margins. The Mn^{II} and Fe^{III} ($3d^5$) ions having five unpaired electrons, as well as Gd^{III} ($4f^7$) ions posses a high magnetic moment. Therefore, their aqua ions cause a substantial shortening of the proton relaxation time in solution. However, the application of metal aqua complexes as contrast agents is limited by their high toxicity. Thus, the LD_{50} values for chlorides of the above-mentioned metals in aqueous solution are 1.4, 1.5, and 1.6 mmol kg^{-1}, respectively.[2]

The calculations for complexes of molar composition Fe^{III} : HEDP = 1 : 1 were carrier out[3] using models of different compositions, including complexonates $Fe(HiL)_i^{-1}$ (i = 0—3), $Fe(OH)_jL^{(1+j)}$ (j = 0—2) and hydroxo complexes $Fe(OH)_k^{3-k}$ (k = 1—4); the Fe^{III} hydrolysis constants were taken from the publication.[4] The formation of insoluble polynuclear complexonates at Fe^{III} concentrations in the range of 10^{-4}—10^{-3} mol dm^{-3} in the presence of excess HEDP was not observed.[3] Apparently, this is attributed to low (millimolar) concentrations of the central ion and ligands. Like other organophosphorus complexones, HEDP tends to form protonated complexes with Fe^{III} even in strongly acidic medium; at pH values corresponding to neutral medium, the solution contains the normal FeL^- complexonate, which is only slightly less stable ($\log\beta$ = 22—23) than the $FeEDTA^-$ complex ($\log\beta$ = 25.1), where EDTA is ethylenediaminetetraacetic acid. A further increase in pH of the solution results in the formation of a monohydroxo complex stable up to pH < 11. The data reported in the study[3] are in agreement with some published data,[4,5] whereas the clearly underestimated stability constants for the normal complexonate were reported in the studies.[6,7]

The review[8] devoted to the use of iron complexes as MRI contrast agents provides evidence that iron(III) complexes with polyaminocarboxylates (including EDTA, diethylenetriaminepentaacetic acid (DTPA), and 1,4,7,10-tetraazacyclodecane-1,4,7,10-tetraacetate (DOTA)) are inefficient in relaxation. For example, at 20 MHz and 40 °C, the relaxation efficiency coefficients REC_1 for complexes with DOTA are 400 mol^{-1} L^{-1} s^{-1}.[9] Nevertheless, Fe^{III}—EDTA complexes were supposed to be suitable for MRI.[10]

The $MnHL_2^{5-}$, $MnH_2L_2^{4-}$, and MnL^{2-} systems are of particular interest among those discussed in the study.[11] The modeling of administration of these complexes to the human body, which is accompanied by an approximately thousand-fold dilution, demonstrated that MnL^{2-} is the most stable complex in the series under consideration. The formation of other complexes is not observed under these conditions, and the concentration of free manganese(II)

Published in Russian in *Izvestiya Akademii Nauk. Seriya Khimicheskaya,* No. 8, pp. 1369—1375, August, 2018.

in the blood does not exceed the maximum allowable concentration (MAC) for drinking water.[12] The relaxation efficiency coefficient REC_2, evaluated as $(C_{Me}{}^{n+} \cdot T_{1(2)})^{-1}$,[13] is ~2500 mol^{-1} L^{-1} s^{-1}, which is sufficient for a contrast agent.

It should be noted that the complexation has not been studied earlier for Fe^{III}—Mn^{II}—HEDP systems. For the Fe^{III}—HEDP system, substantially different complexation patterns and equilibrium constants were reported in the literature.[3—5,14] Rather stable complexes with a high relaxation efficiency coefficient (REC_2) characterized by the spin-spin relaxation time (T_2) were observed in the Mn^{II}—HEDP system.[11]

The aim of this work is to identify highly reactive heteronuclear Mn^{II} and Fe^{III} complexes based on HEDP and determine the stability constants of the species that are formed in the Mn^{II}—Fe^{III}—HEDP system in order to evaluate the possibility of using these complexes in MRI. Due to a combination of two or more paramagnetic ions in a heteronuclear complex, these compounds would be expected to be versatile contrast agents, and this combination will enhance their efficiency in MRI due to an increase in relaxivity.

In this work, we studied the Fe^{III}—HEDP system and the heteronuclear Mn^{II}—Fe^{III}—HEDP system by pH potentiometry combined with NMR relaxation. All pH-potentiometric measurements were performed at different metal-to-ligand ratios and a three-fold or higher dilution, which allowed the reliable detection of polynuclear complexes in solution.

Experimental

The proton activity was determined on an Ekspert-001 potentiometer (Russia) with an accuracy of 0.005 pH units; the pH meter was calibrated with standard aqueous buffer solutions.

The NMR proton relaxation times were measured with a Minispec MQ20 NMR relaxometer (Bruker) operating at 19.75 MHz. The temperature (25 °C) was maintained constant with a Haake DC10 cryo thermostat (Thermo Electron). The time T_2 was measured using Han's technique (90°—τ—180°) and the Carr—Purcel—Meiboom—Gill (CPMG) pulse sequence (90°—τ—(180°—2τ)n, where n is the number of 180° pulses).[15] All experiments were performed in at least triplicate.

The concentration of a HEDP (Sigma) solution was measured by pH-metric titration with a carbonate-free KOH solution, the concentration of which was determined by the titration with a Fixanal solution (0.1 N HCl solution). The concentration of a solution of manganese nitrate (reagent grade) was determined by titration with an EDTA solution using Eriochrome Black T as an indicator in an ammonium buffer solution.[16] Iron nitrate (reagent grade) solutions were titrated with an EDTA solution in the presence of sulfosalicylic acid as an indicator of the equivalence point.[17]

The test titration using the displacement of carbon dioxide gas from the titrated solution by purging with argon showed that this procedure does not lead to a considerable difference in the titration curves. Therefore, the main data were obtained under an air atmosphere. The conclusion that there is no need to purge with argon was also drawn in the study,[18] where the acid-base behavior of alendronic acid (amine-functionalized HEDP) was examined at concentrations higher than 10^{-2} mol L^{-1}.

The experimental dependences of physicochemical properties on the composition of solutions were processed with the CPESSP program (Complex formation Parameters of Equilibria in Solutions with Solid Phases).[19] The program allows the processing of data obtained by different methods (NMR, pH-metry, polarimetry, spectrophotometry, *etc.*) and can be employed to calculate the ionic strength and activity coefficients at each titration point. The characteristic parameter of the data follows the additivity rule. The program searches for the minimum of the functional F by an iterative procedure.[11]

Results and Discussion

The Fe^{III}—HEDP system. We performed pH-metric titration of this system (Fig. 1) and obtained pH dependences of the spin-spin relaxation efficiency coefficient (Fig. 2) at different concentrations given in Tables 1 and 2, respectively.

The pH-metric titration data were processed by mathematical modeling, which allowed us to correctly describe the Fe^{III}—HEDP system (Table 3); the Fisher criterion was 0.54 (see Fig. 1).

Figure 2 displays the NMR relaxation data for the ratios of the components of the system given in Table 2. It should be noted that the REC_2 value is significantly lower than that for the aqua ion even in strongly acidic medium at pH close to zero,[15] which is unambiguous evidence[13,15] that iron(III) forms complexes with HEDP. The final stoichiometric matrix (see Table 3) adequately describes the NMR data.

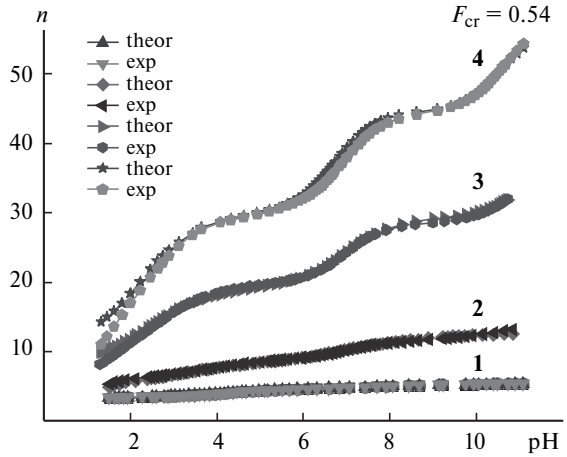

Fig. 1. Theoretical (theor) and experimental (exp) plots of the Bjerrum function n (based on the metal) *vs* pH for the Fe^{III}—HEDP system (in calculations, the ligands was used as the first basis species). The experimental conditions and their numbering are given in Table 1.

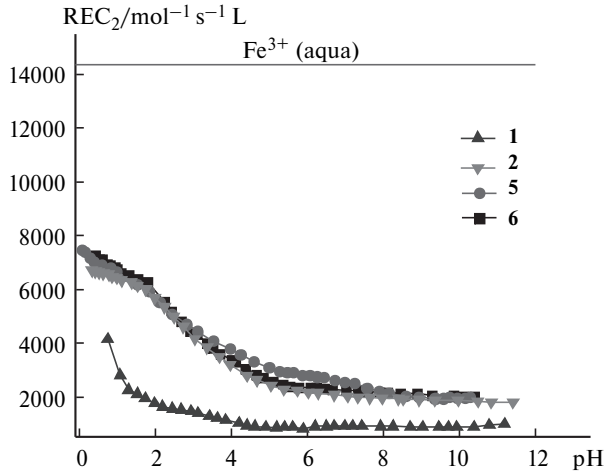

Fig. 2. Experimental plots of the spin-spin relaxation efficiency coefficient REC_2 *vs* pH for the Fe^{III}—HEDP system at different component ratios. The experimental conditions and their numbering are given in Table 2.

Table 1. Concentration conditions for the Fe^{III}—HEDP system (V_{init} = 25 mL, T = 25 °C) studied by pH potentiometry

Run	$C°_{Fe^{III}}$	$C°_{HEDP}$ /mol L^{-1}	$C°_{KOH}$
1	$2.268 \cdot 10^{-2}$	$2.528 \cdot 10^{-2}$	$1.243 \cdot 10^{-1}$
2	$1.811 \cdot 10^{-2}$	$5.891 \cdot 10^{-2}$	$2.611 \cdot 10^{-1}$
3	$9.101 \cdot 10^{-3}$	$8.047 \cdot 10^{-2}$	$9.748 \cdot 10^{-2}$
4	$9.101 \cdot 10^{-3}$	$1.288 \cdot 10^{-1}$	$9.748 \cdot 10^{-1}$

Table 2. Concentration conditions for the Fe^{III}—HEDP system studied by NMR, T = 25 °C

Run	$C°_{Fe^{III}}$ /mol L^{-1}	$C°_{HEDP}$
1	$2.091 \cdot 10^{-2}$	$2.528 \cdot 10^{-2}$
2	$1.811 \cdot 10^{-2}$	$5.891 \cdot 10^{-2}$
5	$9.101 \cdot 10^{-3}$	$7.252 \cdot 10^{-2}$
6	$9.101 \cdot 10^{-3}$	$3.359 \cdot 10^{-2}$

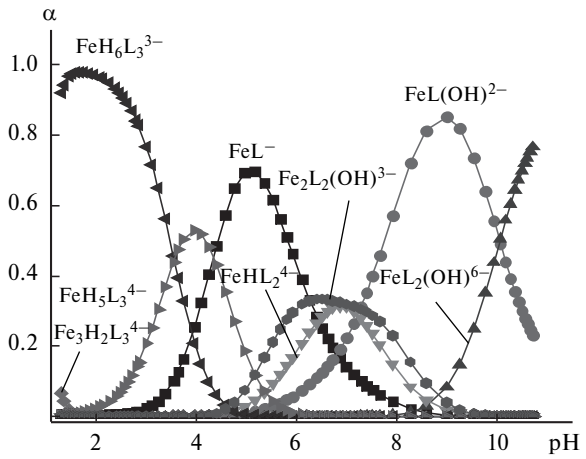

Fig. 3. Plots of accumulation fractions of different forms (based on the metal) *vs* pH of the medium at $C_{Fe^{III}} = 9.101 \cdot 10^{-3}$ mol L^{-1} and $C_{HEDP} = 8.047 \cdot 10^{-2}$ mol L^{-1} (see Table 1, run **3**).

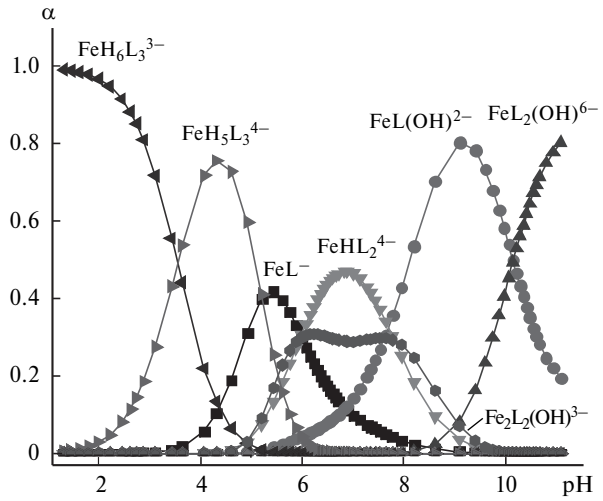

Fig. 4. Plots of accumulation fractions of different forms (based on the metal) *vs* pH of the medium at $C_{Fe^{III}} = 9.101 \cdot 10^{-3}$ mol L^{-1} and $C_{HEDP} = 1.288 \cdot 10^{-1}$ mol L^{-1} (see Table 1, run **4**).

We also obtained pH dependences of the accumulation fractions of the complexes (based on the metal) at different concentrations (Figs 3—6).

Table 3. Stoichiometric matrix, formation constants (K_p), and stability constants ($\log\beta_{stab}$) in the Fe^{III}—HEDP system, F_{cr} = 0.54

Run	Equilibrium	n	$\log K_p$, $\delta \leqslant 0.14$	$\log\beta_{stab}$, $\delta \leqslant 0.3$
1	$Fe^{3+} + H_4L \rightleftharpoons FeL^- + 4\ H^+$	4.0	10.18	33.9
2	$Fe^{3+} + H_4L \rightleftharpoons FeL(OH)^{2-} + 5\ H^+$	5.0	3.02	40.7
3	$Fe^{3+} + 2\ H_4L \rightleftharpoons FeL_2(OH)^{6-} + 9\ H^+$	9.0	−19.39	41.9
4	$Fe^{3+} + 2\ H_4L \rightleftharpoons FeHL_2^{4-} + 7\ H^+$	7.0	−0.11	35.7
5	$3\ Fe^{3+} + 3\ H_4L \rightleftharpoons Fe_3H_2L_3^- + 10\ H^+$	3.3	42.30	90.3
6	$Fe^{3+} + 3\ H_4L \rightleftharpoons FeH_6L_3^{3-} + 6\ H^+$	6.0	12.17	26.2
7	$Fe^{3+} + 3\ H_4L \rightleftharpoons FeH_5L_3^{4-} + 7\ H^+$	7.0	7.97	29.5
8	$2\ Fe^{3+} + 2\ H_4L \rightleftharpoons Fe_2L_2(OH)^{3-} + 9\ H^+$	4.5	16.08	77.4

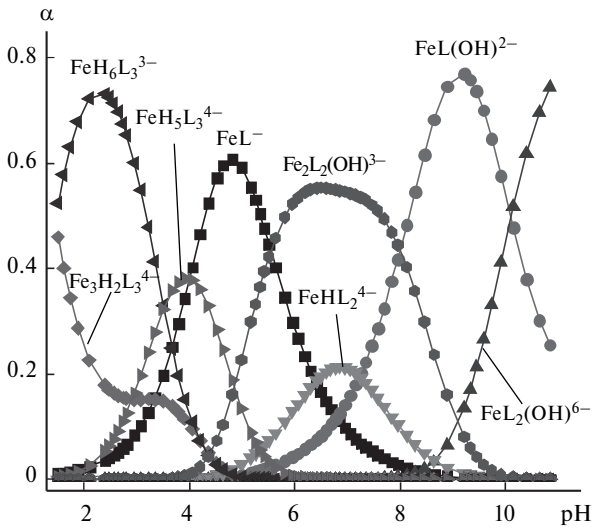

Fig. 5. Plots of accumulation fractions of different forms (based on the metal) *vs* pH of the medium at $C_{Fe}^{III} = 1.811 \cdot 10^{-2}$ mol L^{-1} and $C_{HEDP} = 5.891 \cdot 10^{-2}$ mol L^{-1} (see Table 1, run **2**).

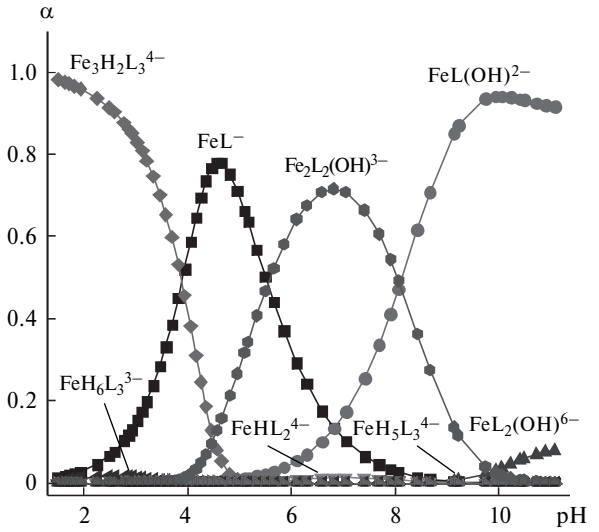

Fig. 6. Plots of accumulation fractions of different forms (based on the metal) *vs* pH of the medium at $C_{Fe}^{III} = 2.268 \cdot 10^{-2}$ mol L^{-1} and $C_{HEDP} = 2.528 \cdot 10^{-2}$ mo L^{-1} (see Table 1, run **1**).

It was found that at metal-to-ligand ratios equal to 1 : 1 and 1 : 3, the species with the metal-to-ligand ratios of 1 : 1 and 3 : 3 (FeL^- and $Fe_3H_2L_3^{3-}$) are predominantly accumulated in the acidic region, while the hydroxo species $FeL_2(OH)^{6-}$ and $FeL(OH)^{2-}$ exist in the alkaline regions.

In the presence of a considerable excess of the ligand, the $FeH_5L_3^{4-}$ and $FeH_6L_3^{3-}$ species are predominantly accumulated in the acidic region; in the alkaline region, $FeL_2(OH)^{6-}$ and $FeL(OH)^{2-}$ are formed.

In the case of the metal-to-ligand ratio equal to 2 : 2, the $Fe_3H_2L_3^{4-}$ complex is accumulated in the acidic region, whereas the $FeL(OH)^{2-}$ complex still prevails in the alkaline region.

It should be noted that the compositions of the manganese(II) complexes[11] greatly differ from those of the iron(III) complexes (see Table 3). There is the only common species of composition MeL^{Z-4}, the iron(III) complex being much more stable (log β = 33.7) than the manganese(II) complex (log β = 11.2). This is apparently due to the significantly smaller ionic radius of Fe^{III} (0.78 Å *vs* 0.97 Å for Mn^{II}),[20] which leads to spatial differences in the coordination of ligand donor groups. The FeL^- complex that is more stable than MnL^{2-} has a higher ionic potential (Z/r_{ion}) (3.85 *vs* 2.06 for Mn^{II}). The latter parameter (Z/r_{ion}) is responsible for the presence of the iron hydroxo complexes $Fe_2L_2(OH)^{3-}$, $FeL(OH)^{2-}$, and $FeL_2(OH)^{6-}$.

The modeling of the administration of these complexes to the human body, which is \accompanied by an approximately thousand-fold dilution, showed that $FeL(OH)^{2-}$ is the most stable complex at pH 7.4 (pH value in human blood) The formation of the other complexes is not observed under these conditions, and the concentration of free iron(III) in the blood is below the MAC for iron in drinking water.[12] It should be noted that the relaxation efficiency coefficient REC_2 (~1100 mol^{-1} s^{-1} L^{-1}) is insufficiently high for a contrast agent.

The Fe^{III}—Mn^{II}—HEDP system. We performed pH-metric titration of this system (Fig. 7) and obtained pH dependences of the spin-spin relaxation efficiency coefficient (Fig. 8) at different concentrations given in Tables 4 and 5. The experimental curves of pH-metric titration for the system (Fig. 9) and the curves calculated using the matrices, which were determined earlier for homonuclear systems composed of species of manganese(II)[11] and iron(III) complexes (see Table 3), provide unambiguous evidence for the formation of heteronuclear iron manganese complexes.

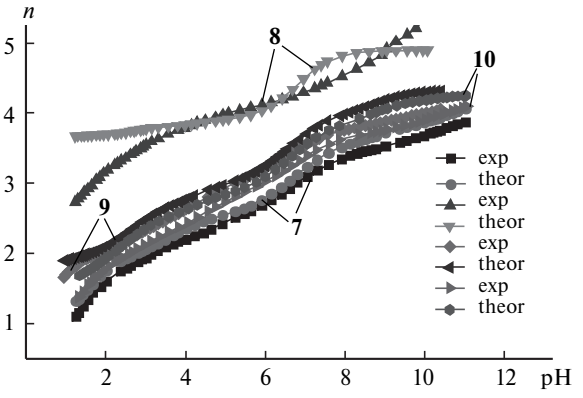

Fig. 7. Experimental (exp) and theoretical (theor) (calculated without taking into account the formation of heteronuclear structures) plots of the Bjerrum function (n) *vs* pH for the Fe^{III}—Mn^{II}—HEDP system. The experimental conditions and their numbering are given in Table 4.

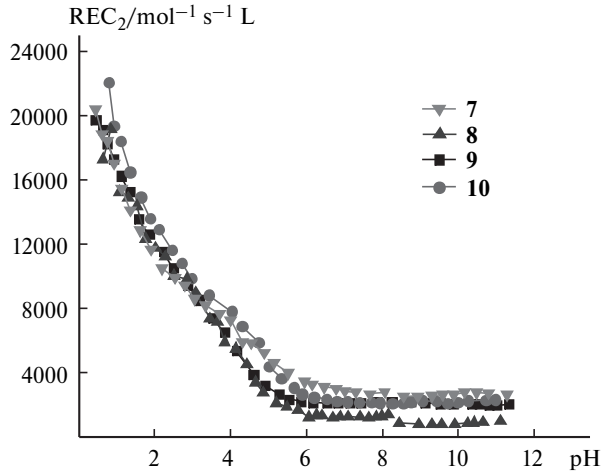

Fig. 8. Experimental plots of the spin-spin relaxation efficiency coefficient REC_2 *vs* pH for the Fe^{III}—HEDP system for different ratios given in Table 5.

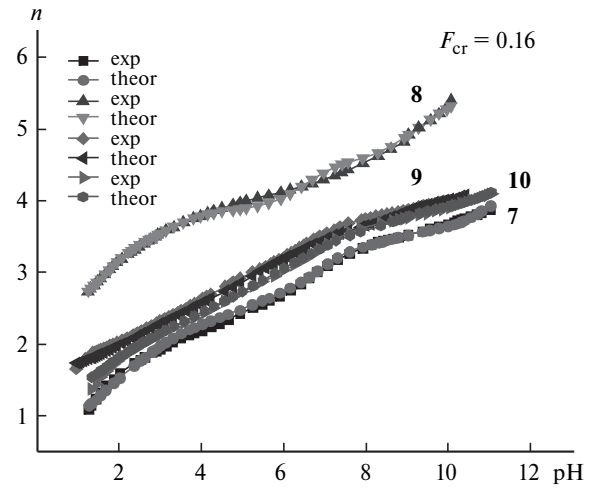

Fig. 9. Theoretical (theor) and experimental (exp) plots of the Bjerrum function (based on the ligand) *vs* pH under the conditions given in Table 4.

A comparison of the magnetic relaxation data[11] for homonuclear systems (see Fig. 2) with those for the heteronuclear iron manganese system (see Fig. 8) also attests to the formation of heteronuclear complexes. The REC_2 value was calculated using the sum of the concentrations of paramagnetic components ($REC_2 = [(C_{Mn^{II}} + C_{Fe^{III}}) \cdot T_2]^{-1}$).

The acid-base properties of HEDP[21] and the addition of different heteronuclear species to the matrix along with the available iron(III) complexes (Table 3) and manganese(II) complexes[22] substantially improved the general pattern. This system was correctly described by mathematical modeling; the Fisher criterion (F) was 0.16 (see Fig. 9).

Table 4. Concentration conditions for the Fe^{III}—Mn^{II}—HEDP system at V_{start} = 25 mL (pH potentiometry), T = 25 °C

Run	$C^{\circ}_{Fe^{III}}$	$C^{\circ}_{Mn^{II}}$	C°_{HEDP}	C°_{KOH}
	mol L^{-1}			
7	$0.911 \cdot 10^{-2}$	$1.071 \cdot 10^{-2}$	$5.052 \cdot 10^{-2}$	$2.113 \cdot 10^{-1}$
8	$2.268 \cdot 10^{-2}$	$2.137 \cdot 10^{-2}$	$2.522 \cdot 10^{-2}$	$1.243 \cdot 10^{-1}$
9	$2.268 \cdot 10^{-2}$	$2.137 \cdot 10^{-2}$	$6.728 \cdot 10^{-2}$	$2.735 \cdot 10^{-1}$
10	$0.911 \cdot 10^{-2}$	$1.071 \cdot 10^{-2}$	$3.372 \cdot 10^{-2}$	$1.243 \cdot 10^{-1}$

Table 5. Concentration conditions for the Fe^{III}—Mn^{II}—HEDP system studied by NMR, T = 25 °C

Run	$C^{\circ}_{Fe^{III}}$	$C^{\circ}_{Mn^{II}}$	C°_{HEDP}
	mol L^{-1}		
7	$1.049 \cdot 10^{-2}$	$1.071 \cdot 10^{-2}$	$5.892 \cdot 10^{-2}$
8	$2.091 \cdot 10^{-2}$	$1.962 \cdot 10^{-2}$	$2.522 \cdot 10^{-2}$
9	$2.091 \cdot 10^{-2}$	$1.962 \cdot 10^{-2}$	$6.728 \cdot 10^{-2}$
10	$1.049 \cdot 10^{-2}$	$1.071 \cdot 10^{-2}$	$3.792 \cdot 10^{-2}$

The application of the matrix obtained from the pH-metric titration data to the NMR relaxation data confirmed that the matrix is adequate and mathematically reliable. The final data on the stoichiometry and formation constants of the corresponding forms are given in Table 6. The accumulation fractions of the species (based on the ligand) depending on the concentration conditions are shown in Figs 10—13.

Therefore, in the Mn^{II}—HEDP system, there are the following polynuclear species of composition 2 : 2 with different degrees of deprotonation: $Mn_2H_3L_2^-$, $Mn_2H_2L_2^{2-}$, and $Mn_2HL_2^{3-}$.[11] In the Fe^{III}—HEDP system, the complexes of compositions 2 : 2 and 3 : 3 are formed: $Fe_2L_2(OH)^{3-}$ and $Fe_3H_2L_3^{3-}$ (see Table 3). The hetero-

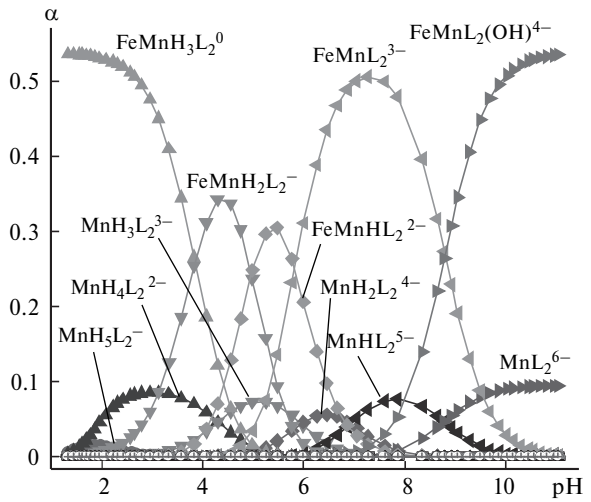

Fig. 10. Plots of accumulation fractions (based on the ligand) *vs* pH of the medium at $C_{Fe^{III}} = 0.911 \cdot 10^{-2}$ mol L^{-1}, $C_{Mn^{II}} = 1.071 \cdot 10^{-2}$ mol L^{-1}, and $C_{HEDP} = 3.372 \cdot 10^{-2}$ mol L^{-1} (see Table 4, run **10**).

Table 6. Stoichiometric matrix, formation constants (log K_p), and stability constants (log β_{stab}) in the Fe^{III}—Mn^{II}—HEDP system, $F_{cr} = 0.16$

Run	Equilibrium	*n*	logK_p, $\delta \leqslant 0.17$	log β_{stab}, $\delta \leqslant 0.3$
1	$Fe^{3+} + H_4L \rightleftharpoons FeL^- + 4\ H^+$	4.0	10.18	33.9
2	$Mn^{2+} + 2\ H_4L \rightleftharpoons MnH_5L_2^- + 3\ H^+$	3.0	−0.78	5.5
3	$Mn^{2+} + 2\ H_4L \rightleftharpoons MnH_4L_2^{2-} + 4\ H^+$	4.0	−2.50	6.8
4	$Mn^{2+} + 2\ H_4L \rightleftharpoons MnH_3L_2^{3-} + 5\ H^+$	5.0	−7.20	9.7
5	$Mn^{2+} + 2\ H_4L \rightleftharpoons MnH_2L_2^{4-} + 6\ H^+$	6.0	−13.77	10.6
6	$Mn^{2+} + 2\ H_4L \rightleftharpoons MnHL_2^{5-} + 7\ H^+$	7.0	−21.49	14.4
7	$Mn^{2+} + 2\ H_4L \rightleftharpoons MnL_2^{6-} + 8\ H^+$	8.0	−31.28	16.1
8	$Fe^{3+} + H_4L \rightleftharpoons FeL(OH)^{2-} + 5\ H^+$	5.0	3.02	40.7
9	$Fe^{3+} + Mn^{2+} + H_4L \rightleftharpoons FeMnL(OH)^0 + 5\ H^+$	5.0	5.79	43.5
10	$Fe^{3+} + Mn^{2+} + H_4L \rightleftharpoons FeMnL(OH)_2^- + 6\ H^+$	6.0	−3.65	48.0
11	$Fe^{3+} + Mn^{2+} + 2\ H_4L \rightleftharpoons FeMnH_3L_2^0 + 5\ H^+$	2.5	28.75	45.6
12	$Fe^{3+} + Mn^{2+} + 2\ H_4L \rightleftharpoons FeMnH_2L_2^- + 6\ H^+$	3.0	24.82	49.2
13	$Fe^{3+} + Mn^{2+} + 2\ H_4L \rightleftharpoons FeMnHL_2^{2-} + 7\ H^+$	3.5	19.60	55.5
14	$Fe^{3+} + Mn^{2+} + 2\ H_4L \rightleftharpoons FeMnL_2^{3-} + 8\ H^+$	4.0	13.34	60.7
15	$Fe^{3+} + Mn^{2+} + 2\ H_4L \rightleftharpoons FeMnL_2(OH)^{4-} + 9\ H^+$	4.5	3.90	65.2
16	$2\ Fe^{3+} + Mn^{2+} + 3\ H_4L \rightleftharpoons Fe_2MnH_4L_3^0 + 8\ H^+$	2.7	43.02	72.1
17	$2\ Fe^{3+} + Mn^{2+} + 3\ H_4L \rightleftharpoons Fe_2Mn\ H_3L_3^- + 9\ H^+$	3.0	42.09	78.6
18	$2\ Fe^{3+} + Mn^{2+} + 3\ H_4L \rightleftharpoons Fe_2MnH_2L_3^{2-} + 10\ H^+$	3.3	40.13	88.2
19	$2\ Fe^{3+} + Mn^{2+} + 3\ H_4L \rightleftharpoons Fe_2MnHL_3^{3-} + 11\ H^+$	3.7	36.26	95.8
20	$2\ Fe^{3+} + Mn^{2+} + 3\ H_4L \rightleftharpoons Fe_2MnL_3^{4-} + 12\ H^+$	4.0	27.11	98.2

nuclear complexes in this system (see Table 6) are both binuclear ($FeMnH_3L_2^0$, $FeMnH_2L_2^-$, $FeMnHL_2^{2-}$, $FeMnL(OH)^0$, $FeMnL(OH)_2^-$, $FeMnL_2^{3-}$, $FeMnL_2(OH)^{4-}$) and trinuclear ($Fe_2MnH_4L_3^0$, $Fe_2MnH_3L_3^-$, $Fe_2MnH_2L_3^{2-}$, $Fe_2MnHL_3^{3-}$).

Apparently, binuclear manganese(II) species serve as the basis for heterobinuclear complexes. Three of these binuclear forms coincide in pairs even with respect to the degree of ligand deprotonation ($Mn_2H_3L_2^-$, $Mn_2H_2L_2^{2-}$, $Mn_2HL_2^{3-}$ and $FeMnH_3L_2^0$, $FeMnH_2L_2^-$, $FeMnHL_2^{2-}$). Iron(III) gives only the trinuclear complex $Fe_3H_2L_3^{3-}$; however, in the presence of manganese(II) ions in solution, the number of heterotetranucelar complexes increases to four, the species having different degrees of ligand deprotonation. Heteronuclear complexes are predominant regarding the accumulation fractions under all the concentration conditions used, particularly, at the concentrations of complex-forming cations equal to ~0.02 mol L^{-1} (see Figs 12 and 13). At $C_{Mn^{II}} \sim C_{Fe^{III}} \sim 0.01$ mol L^{-1} in the presence of excess HEDP, manganese(II) complexes of composition 1 : 2 with different degrees of ligand deprotonation are accumulated in minor fractions (see Figs 10 and 11).

The diversity and high stability (Table 7) of heteronuclear iron manganese complexes apparently provide

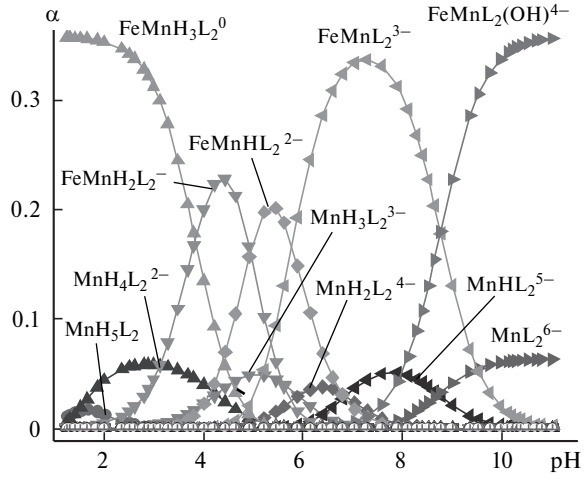

Fig. 11. Plots of accumulation fractions (based on the ligand) *vs* pH of the medium at $C_{Fe^{III}} = 0.911 \cdot 10^{-2}$ mol L^{-1}, $C_{Mn^{II}} = 1.071 \cdot 10^{-2}$ mol L^{-1}, and $C_{HEDP} = 5.052 \cdot 10^{-2}$ mol L^{-1} (see Table 4, run **7**).

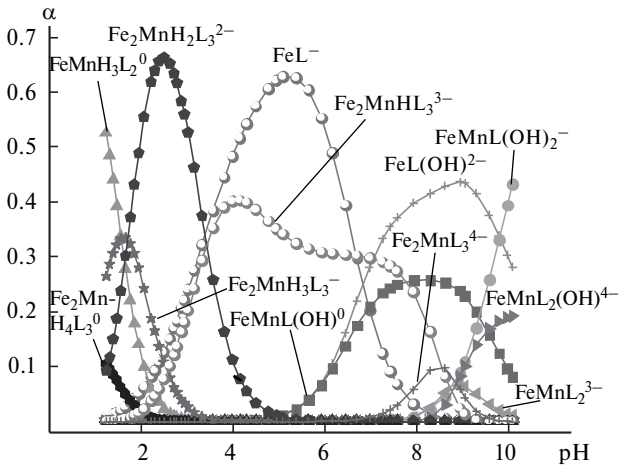

Fig. 12. Plots of accumulation fractions (based on the ligand) *vs* pH of the medium at $C_{Fe^{III}} = 2.268 \cdot 10^{-2}$ mol L^{-1}, $C_{Mn^{II}} = 2.137 \cdot 10^{-2}$ mol L^1, and $C_{HEDP} = 2.522 \cdot 10^{-2}$ mol L^{-1} (see Table 4, run **8**).

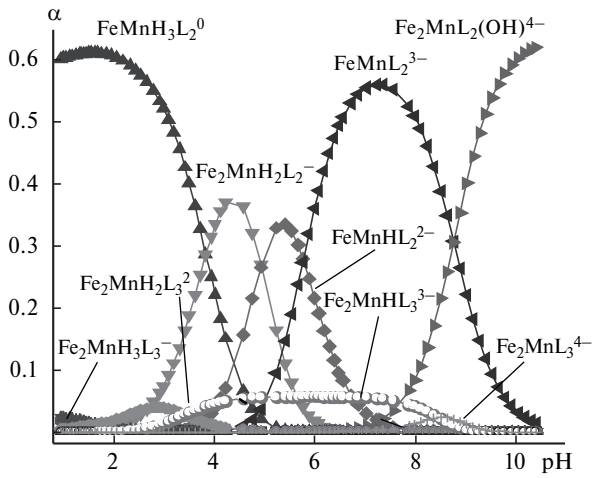

Fig. 13. Plots of accumulation fractions (based on the ligand) *vs* pH of the medium at $C_{Fe^{III}}=2.268\cdot10^{-2}$ mol L^{-1}, $C_{Mn^{II}} = 2.137\cdot10^{-2}$ mol L^{-1}, and $C_{HEDP} = 6.728\cdot10^{-2}$ mol L^{-1} (see Table 4, run **9**).

Table 7. Relative stability ($\log\beta_{stab}$) of homo- and heterobinuclear related complexes

Complex	$\log\beta_{stab}$	Complex	$\log\beta_{stab}$
$Mn_2H_3L_2^-$	12.7	$FeMnH_3L_2^0$	45.6
$Mn_2H_2L_2^{2-}$	15.9	$FeMnH_2L_2^-$	49.2
$Mn_2HL_2^{3-}$	21.2	$FeMnHL_2^2$	55.5

a favorable combination of sizes and ionic potentials of complex-forming cations — iron(III) and manganese(II), resulting in the optimal spatial configuration of the complexes and a lower Gibbs free energy compared to homonuclear systems.

The modeling of the administration of a solution with concentrations $C_{Fe^{III}}=0.0227$ mol L^{-1}, $C_{Mn^{II}}=0.0214$ mol L^{-1}, and $C_{HEDP} = 0.0252$ mol L^{-1} to the human body, which is accompanied by approximately a thousand-fold dilution, showed that the $MnH_3L_2^{3-}$ (39%), $FeMnH_3L_2^0$ (31%), and $Fe_2MnHL_3^{3-}$ (30%) complexes co-exist at pH 7.4 (the value for the human blood). The formation of the other complexes at a thousand-fold dilution is not observed, and the concentrations of free iron(III) and manganese(II) cations are below the MAC for these cations in drinking water.[12] The average relaxation efficiency coefficient REC_2 is ~2000 $mol^{-1}\ s^{-1}\ L^{-1}$, which is rather large for a contrast agent.

References

1. R. R. Amirov, *Soedineniya metallov kak magnitno-relaksatsionnye zondy dlya vysokoorganizovannykh sred. Primenenie v MR-tomografii i khimii rastvorov* [*Metal Compounds as Magnetic Relaxation Probes for Highly Organized Media. Application in MR Imaging and Solution Chemistry*], Novoe znanie, Kazan, 2005, 316 pp. (in Russian).
2. US Pat. 5494656; *The University of Toledo*, 1996, **08**, 406356.
3. T. N. Kropacheva, A. N. Pagin, V. I. Kornev, *Vestn. Udmurtskogo un-ta* [*Bull. Udmurt. Univ.*], 2012, **4**, 64 (in Russian).
4. P. Gans, A. Sabatini, A. Vacca, *Talanta*, 1996, **43**, 1739—1753.
5. E. Gumienna-Kontecka, R. Silvagni, R. Lipinski, M. Lecoyvey, F. C. Marincola, G. Crisponi, V. M. Nurchi, Y. Leroux, H. Kozlowski, *Inorg. Chim. Acta*, 2002, **339**, 111—118.
6. S. Lacour, V. Deluchat, J. C. Bollinger, B. Serpaud, *Talanta*, 1998, **46**, 999—1009.
7. N. M. Dyatlova, V. Ya. Temkina, K. I. Popov, *Kompleksony i kompleksonaty metallov* [*Complexones and Metal Complexonates*], Khimiya, Moscow, 1988, 544 pp. (in Russian).
8. N. Richardson, J. A. Davies, B. Raduchel, *Polyhedron*, 1999, **18**, 2457—2482.
9. C. A. Chang, L. C. Francesconi, M. F. Malley, K. Kumar, J. Z. Gougoutas, M. F. Tweedle, *Inorg. Chem.*, 1993, **32**, 3501—3508.
10. O. Yu. Borodin, Ph. D. (Med.) Thesis, Cardiology Research Institute, Tomsk National Research Medical Center, Siberian Branch of the Russian Academy of Medical Sciences, Tomsk, 2004, p. 25 (in Russian).
11. O. V. Bogatyrev, A. F. Yamaltdinova, F. V. Devyatov, *Uchen. zap. Kazan. un-ta. Ser. estestv. nauki* [*Proceedings of Kazan University, Natural Sci. Series*], 2016, **158**, 44—54 (in Russian).
12. *Vrednye khimicheskie veshchestva. Neorganicheskie soedineniya V-VIII grupp. Spravochnik* [*Harmful Chemical Substances. Inorganic Compounds of Elements of V—VIII Groups. Handbook*], Ed. V. A. Filov, Khimiya, Leningrad, 1989, 592 pp. (in Russian).
13. A. A. Popel′, *Magnitno-relaksatsionnyi metod analiza neorganicheskikh veshchestv* [*Magnetic Relaxation Method for Analysis of Inorganic Substances*], Khimiya, Moscow, 1978, 222 pp. (in Russian).
14. V. P. Vasil′ev, E. V. Kozlovskii, V. V. Serdyukov, *Russ. J. Inorg. Chem.*, 1990, **35**, 373—376.
15. A. A. Vashman, I. S. Pronin, *Yadernaya magnitnaya relaksatsiya i ee primenenie v khimii* [*Nuclear Magnetic Relaxation and Its Applications in Chemistry*], Nauka, Moscow, 1979, 236 pp. (in Russian).
16. V. N. Alekseev, *Kolichestvennyi analiz* [*Quantitative Analysis*], Vysshaya shkola, Moscow, 1972, 504 pp. (in Russian).
17. F. Umland, A. Janssen, D. Thierig, G. Wunsch, *Theorie und praktische Anwendung von Komplexbildnern*, Akademische Verlagsgesellschaft, Frankfurt Am Main, 1971, 759 pp.
18. A. P. Boichenko, V. V. Markov, A. L. Ivashchenko, E. Yu. Spirina, L. P. Loginova, *Visn. Kharkiv. nats. un-tu* [*Bull. Kharkiv Univ.*], 2007, **770**, 62—69 (in Russian).
19. Yu. I. Sal′nikov, A. N. Glebov, F. V. Devyatov, *Poliyadernye kompleksy v rastvorakh* [*Polynuclear Complexes in Solutions*], Izd-vo Kazanskogo un-ta, Kazan, 1989, 288 pp. (in Russian).
20. J. E. Huheey, *Inorganic Chemistry. Principles of Structure and Reactivity*, Harper & Row, New York, 1983, 936 pp.
21. D. R. Musin, A. V. Rubanov, F. V. Devyatov, *Uchen. zap. Kazan. un-ta. Ser. estestv. nauki* [*Proceedings of Kazan University, Natural Sci. Series*], 2011, **153**, 40—47 (in Russian).
22. F. V. Devyatov, O. V. Bogatyrev, G. I. Zaripova, *Russ. Chem. Bull.*, 2017, **66**, 2090.

Received February 8, 2018;
in revised form May 22, 2018;
accepted May 23, 2018